Langmuir

Article

pubs.acs.org/Langmuir

Methyl Oleate-Capped Upconverting Nanocrystals: A Simple and General Ligand Exchange Strategy To Render Nanocrystals Dispersible in Aqueous and Organic Medium

Brahmaiah Meesaragandla, Venkata N. K. B. Adusumalli, and Venkataramanan Mahalingam*

Department of Chemical Sciences, Indian Institute of Science Education and Research, Kolkata 741252, India

Supporting Information

ABSTRACT: We report a simple and general ligand exchange strategy to functionalize the nanocrystals with both hydrophobic and hydrophilic ligands. This is achieved by first capping the Er/Yb-doped $NaYF_4$ nanocrystals with a weak ligand such as methyl oleate and subsequently ligand exchanged with various organic ligands which can strongly coordinate to the surface of the nanocrystals. The method involves only a simple stirring or sonication of the nanocrystals dispersion with the ligands of interest. Dicarboxylic acids such as sebacic acid, adipic acid, succinic acid, and malonic acid-functionalized nanocrystals which are difficult to achieve via thermal decomposition method were easily prepared by this ligand exchange strategy. In addition, low boiling point ligands like hexanoic acid can easily be coated over the surface of the Er/Yb-doped $NaYF_4$ nanocrystals. Both size and shape of the nanocrystals were preserved after the ligand exchange process. The methyl oleate-capped Er/Yb-doped $NaYF_4$ nanocrystals display strong upconversion emission after ligand exchanged with hydrophobic and hydrophilic molecules. The high stability of the nanocrystals after ligand exchange process is verified by performing time-dependent luminescent measurements at different pH, buffers, etc.

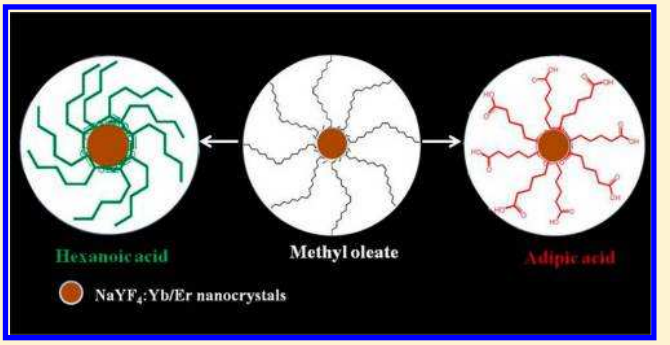

1. INTRODUCTION

Lanthanide (Ln^{3+})-doped nanomaterials receive huge research interest due to their sharp intra 4f−4f transitions which span a wide spectral region.[1−5] The sharp electronic transitions along with their long luminescence lifetimes have been explored for various applications like phosphors for LEDs,[6−8] solar cells,[9−11] and drug delivery,[12,13] just to mention a few. In addition to Stokes shifted luminescence, some Ln^{3+}-doped materials possess the ability to convert low-energy near-infrared (NIR) transition into high-energy visible ones, via the process known as upconversion.[14−18] Ln^{3+}-doped materials possessing this property find potential use in bioimaging applications.[19−23]

Among various host matrices for Ln^{3+} ions, fluorides find interesting due to their low phonon energy resulting in relatively better luminescence efficiency.[24−28] One of the widely used methods to make fluoride nanoparticles is thermal decomposition method, which involves decomposition of the lanthanide precursors at high temperatures (>300 °C) in the presence of capping ligands such as oleic acid, oleylamine, and recinolic aicd.[29−32] This method allows one to prepare small nanoparticles with good monodispersity.[33,34] However, the hydrophobic nature of the capping ligand demands post-chemical functionalization to render the nanocrystals water dispersible.

There are few reports available on improving the stability of oleic acid capped nanocrystals in water via surface functionalization. One is through steric stabilization by encapsulating the hydrophobic (oleic acid) nanocrystals with amphiphilic polymers.[35] However, the additional layers of amphiphilic polymer considerably increase the size of the particles. The second approach is the encapsulation of hydrophobic nanocrystals with SiO_2.[36] Although achieving silica coating is generally easy and simple, the strong Si−O stretching leads to decrease in the emission intensity. Moreover, achieving uniform coating with size control is tedious as it is usually a trial and error process. Third approach is the direct oxidation of the oleic acid double bond resulting in the COOH groups on the surface of the nanocrystals, but the method involves relatively long reaction time (~48 h).[37,38] It is also possible to make water dispersible nanocrystals by simply removing the oleic acid molecules from the surface of the nanocrystals at low pH using 0.1 M HCl.[39] However, this generally reduces the luminescence efficiency due to the presence of H_3O^+ groups on the surface and the absence of capping ligands. Finally, the ligand exchange strategy where the oleic acid molecules attached to the nanocrystals surface get exchange with ligands which are hydrophilic in nature. For example, polymers such as poly(vinylpyrrolidone), poly(acrylic acid), and poly(allylamine) have been used as ligands for exchange.[40−42] Although the above ligand exchange procedures led to water-dispersible

Received: March 23, 2015
Revised: April 21, 2015

DOI: 10.1021/acs.langmuir.5b01070
Langmuir XXXX, XXX, XXX−XXX

nanocrystals, the reaction rates are usually slow and the reaction is performed at high temperatures. Murray's groups have developed a generalized ligand-exchange strategy to increase the choice of ligands by using nitrosonium tetrafluoroborate ($NOBF_4$) as an intermediate ligand.[43] This strategy involves two steps to transfer hydrophobic colloidal nanocrystals into hydrophilic ones. First, the nanocrystals were exchanged with $NOBF_4$ by stirring the mixture for 30 min followed by exchange of the $NOBF_4$ with suitable capping molecules again under stirring. Finally, the nanocrystals were dispersed in water. Yet there is challenge in developing new ligand exchange routes as most of the reports focus on converting hydrophobic to hydrophilic. In addition, the strong binding of the oleic acid to the nanocrystals surface demand high temperature and long reaction times for the ligand exchange. Our idea is to stabilize the nanocrystals using a weak coordinating ligand such as methyl oleate followed by exchanging them with strong ligands. Here we report for the first time the synthesis of methyl oleate (MO)-capped Yb/Er-doped $NaYF_4$ nanocrystals via the thermal decomposition method. The presence of methyl groups near the carboxyl groups (COO) leads to weak binding of the ligand to the nanocrystals surface. This weak binding favors the ligand exchange with a variety of organic molecules, thus making a general strategy for the ligand exchange to render nanocrystals both water and organic dispersible. For example, exchange of methyl oleate with oleic acid, oleylamine, or hexanoic acid enhances the dispersibility of the nanocrystals in organic solvents whereas exchange with dicarboxylic acid molecules provides hydrophilic functional groups near the surface of the nanocrystals to render them dispersible in aqueous medium. The nanocrystals show strong upconversion emission in both organic and aqueous medium after ligand exchange. Some of the advantages of this ligand exchange strategy are (i) fast and the simple procedure, (ii) capping with ligands possessing low boiling points (ca. hexanoic acid, succinic acid, etc.) which are otherwise difficult to use in thermal decomposition method, (iii) small concentration of ligands is enough for surface modification than that needed for the thermal decomposition method, and (iv) shape and size of the nanocrystals are preserved after exchanged with different ligands. The last point is important because the nature of the capping ligands generally affects the size and shape of the nanocrystals if the ligands are used directly during the synthesis of the nanocrystals.

2. EXPERIMENTAL SECTION

2.1. Materials. Y_2O_3, Yb_2O_3, Er_2O_3, CF_3COONa, methyl oleate (80%), 1-octadecene (90%), D_2O, $CDCl_3$, oleic acid, oleylamine, and hexanoic acid were purchased from Sigma-Aldrich. Ethanol, trifluoroacetic acid, toluene, hexane, oxalic acid, malonic acid, succinic acid, adipic acid, and sebacic acid were purchased from Merck. All chemicals were used without further purification.

2.2. Synthesis of Methyl Oleate-Capped (20%) Yb^{3+}/(2%) Er^{3+}-Doped $NaYF_4$ Nanocrystals. The methyl oleate-capped Yb^{3+}/Er^{3+}-doped $NaYF_4$ nanocrystals were synthesized using the thermal decomposition method.[44,45] Briefly a mixture of 0.78 mmol of Y_2O_3, 0.20 mmol of Yb_2O_3, and 0.02 mmol of Er_2O_3 in 5 mL of trifluoroacetic acid and 5 mL of distilled water were taken in a three neck round-bottom flask and reflexed at 85 °C until clear solution was obtained. The resulting solution was evaporated to dryness. Subsequently 2 mmol of CF_3COONa was added to the flask along with 20 mL each of methyl oleate and 1-octadecene. The slurry was degassed while heated to 120 °C under vacuum for 30 min to remove residual water and oxygen, following which the mixture was heated to 300 °C at a rate of approximately 10 °C/min under an Ar atmosphere. The solution was maintained at this temperature for 1 h under an Ar atmosphere and cooled to room temperature. The nanocrystals were precipitated by ethanol and isolated via centrifugation at 3600 rpm for 10 min. Finally, the isolated methyl oleate-capped Yb^{3+}/Er^{3+}-doped $NaYF_4$ nanocrystals were dried under vacuum for 2 days.

2.3. Surface Modification with Oleic Acid, Oleylamine, and Hexanoic Acid. To exchange methyl oleate-capped nanocrystals with oleic acid, oleylamine, and hexanoic acid, 20 mg of the methyl oleate-capped nanocrystals was added to a 2 mL of the ligand in 5 mL of DCM. The above mixture was sonicated for 10 min followed by the addition of ethanol to precipitate the nanocrystals. The nanocrystals were washed with ethanol and dried under vacuum.

2.4. Surface Modification with Dicarboxylic Acids (Oxalic Acid, Malonic Acid, Succinic Acid, Adipic Acid, and Sebacic Acid). 20 mg of the methyl oleate-capped nanocrystals was added to 10 mL of aqueous solution containing 30 mg of dicarboxylic acids. After vigorous stirring/sonication for 10 min, the resulting mixture was mixed with diethyl ether to remove the methyl oleate by extraction. The Yb/Er-doped $NaYF_4$ nanocrystals were dispersed in water.

2.5. Photostability Studies of the Nanocrystals. To check the photostability of the methyl oleate-capped nanocrystals after ligand exchange with malonic acid, succinic acid, adipic acid, and sebacic acid, the nanocrystals were continuously irradiated with 980 nm laser at a power density of 103 W/cm^2, and the corresponding luminescence spectra were recorded at regular intervals.

2.6. Effect of pH on the Stability of the Nanocrystals. The methyl oleate-capped Yb^{3+}/Er^{3+}-doped $NaYF_4$ nanocrystals after ligand exchange with malonic acid, succinic acid, adipic acid, and sebacic acid were independently taken in different glass vials, and the pH of the colloidal dispersion was adjusted using HCl (1 N) and NaOH (1 N) solutions.

2.7. Effect of Different Biologically Media on the Stability of the Nanocrystals. The dicarboxylic acid-capped Yb^{3+}/Er^{3+}-doped $NaYF_4$ nanocrystals were incubated in two biologically relevant media: (a) cell culture medium (DMEM, glucose and 10% FBS) and (b) PBS (phosphate buffer). The upconversion luminescence intensity and the hydrodynamic diameter of the nanocrystals were monitored for 14 days on a daily basis.

2.8. Characterization. The phase analysis of the as-prepared methyl oleate-capped Yb/Er-codoped $NaYF_4$ nanocrystals was examined by X-ray diffraction (XRD) using a Rigaku-SmartLab X-ray diffractometer with a D/tex ultradetector and Cu Kα source operating at 40 kV and 50 mA; data were collected from 20° to 90° with a step size of 0.02° and a counting time of 2 s per step. TEM measurements were carried out on a UHR-FEG-TEM JEOL JEM 2100 F model using a 200 kV electron source. FT-IR spectra were collected from a PerkinElmer FT-IR spectrometer 1000 with a resolution of 2 cm^{-1} and averaged over four scans. The ^1H NMR spectra of all ligand coated nanocrystals were obtained using a JEOL 400 MHz spectrometer. Upconversion luminescence measurements were performed by exciting the 0.5 wt % nanocrystal dispersion with a 980 nm diode laser from RgBLase LLC, which was coupled to a fiber with core diameter of 100 μm. The emitted light was detected using a Horiba JobinYvon fluorometer equipped with a photomultiplier tube. To remove the scattered excitation light, a long-band-pass filter (495 nm) was used on the excitation side. All upconversion emission spectra were measured with the same slit width and with an excitation laser power of 500 mW. The lifetime measurements were carried out by exciting the samples at 478 nm using pulsed Xe lamp (25 W) integrated with the Horiba JobinYvon fluorometer. DLS measurements were measured using a Malvern Zetasizer nano equipped with a 4.0 mW He−Ne laser operating at λ = 630 nm. All samples were measured in an aqueous system at room temperature with scattering angle of 173°. Size distribution calculated by nano software is derived from a non-negative least-squares (NNLS) analysis.

3. RESULTS AND DISCUSSION

Methyl oleate (MO)-capped Yb/Er-doped $NaYF_4$ nanocrystals were prepared using a thermal decomposition method. Figure

DOI: 10.1021/acs.langmuir.5b01070
Langmuir XXXX, XXX, XXX−XXX

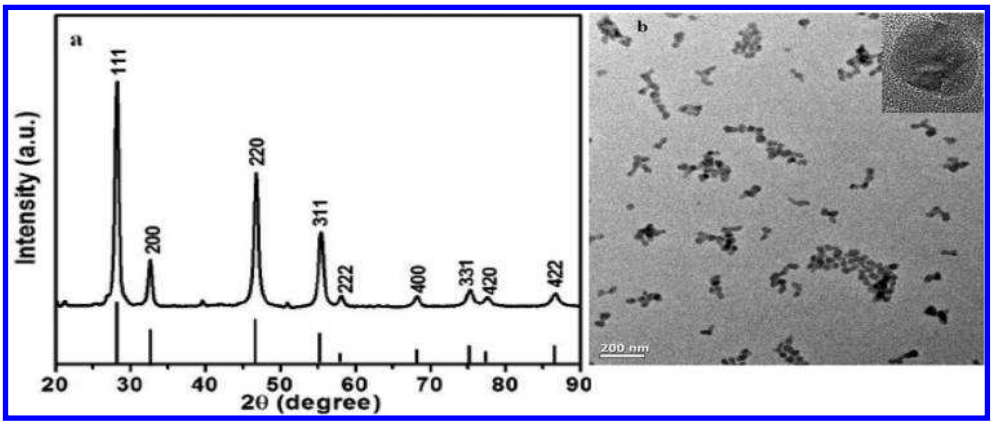

Figure 1. (a) Experimental XRD pattern and (b) TEM image of methyl oleate-capped Yb/Er-doped $NaYF_4$ nanocrystals. The vertical line in (a) is the standard XRD pattern of bulk $NaYF_4$.

1a shows the X-ray diffraction (XRD) pattern collected from the methyl oleate-capped Yb/Er-doped $NaYF_4$ nanocrystals. The peak positions match well with the standard pattern of the bulk α-$NaYF_4$. The weak peaks noted at 41° and 52° are likely due to the presence of hexagonal phase $NaYF_4$. Under similar conditions, when oleic acid molecules were used as capping ligands, formation of α phase $NaYF_4$ nanocrystals is observed (Figure S1). The TEM image of the methyl oleate-capped sEr/Yb-doped $NaYF_4$ nanocrystals is shown in Figure 1b. The average size of the nanocrystals is ~35 nm as suggested by the histogram analysis. This is further supported by the DLS analysis which shows an average size of 43 nm.

The histogram size distribution calculated from TEM and DLS analyses are shown in Figures S2a and 2b, respectively (see Supporting Information). The nanocrystals are partially aggregated due to poor dispersibility in toluene, presumably due to weak binding of the methyl oleate ligands to the surface of the nanocrystals. The binding of the methyl oleate to the surface of the nanocrystals is confirmed by the FTIR and ^1H NMR spectra. Figure 2 shows the FTIR spectra of pure methyl oleate and methyl oleate-capped Er/Yb-doped $NaYF_4$ nanocrystals. The peak observed at 1745 cm^{-1} for pure methyl oleate is assigned to the C═O stretching of $COOCH_3$ group. This peak shifts to 1646 cm^{-1} upon attachment to the nanocrystals surface, suggesting the involvement of −C═O in

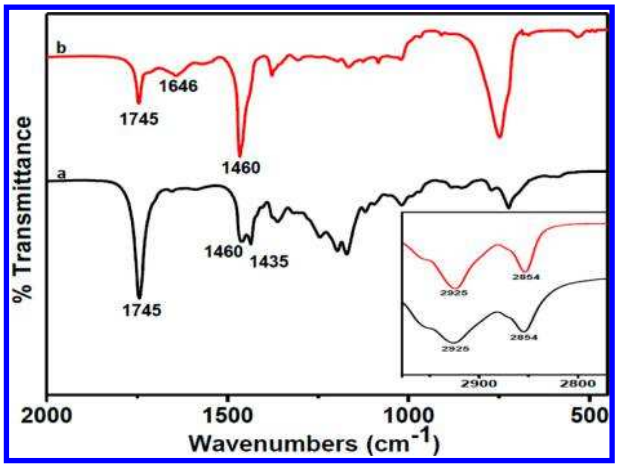

Figure 2. FTIR spectra of (a) pure methyl oleate and (b) methyl oleate-capped Er/Yb-doped $NaYF_4$ nanocrystals. The C−H stretching region is shown in the inset.

binding to the nanocrystals. However, the presence of this peak along with the peak at 1745 cm^{-1} implies the presence of some free methyl oleate ligands. The bands near 2854 and 2925 cm^{-1} are respectively due to symmetric and asymmetric CH_2 stretching vibration modes in methyl oleate (see inset of Figure 2). It is worth to mention that in the case of oleic acid-capped $NaYF_4$ nanocrystals the carbonyl stretching shifted to 1546 cm^{-1} (see Figure S3, Supporting Information). The attachment of MO to the surface of the nanocrystals is further confirmed by ^1H- NMR spectra. The ^1H NMR spectra of pure methyl oleate and the same after capped to Er/Yb-doped $NaYF_4$ nanocrystals are shown in Figures S4 and S5 (Supporting Information). The protons in HC═CH in methyl oleate centered at 5.31−5.33 ppm is preserved upon binding to the nanocrystals.

Figure 3 shows the upconversion emission spectrum of the methyl oleate-capped Er/Yb-doped $NaYF_4$ nanocrystals in

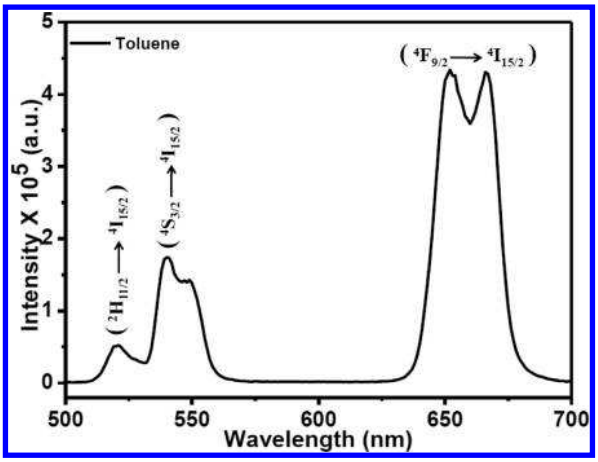

Figure 3. Upconversion (UC) emission spectrum of the methyl oleate-capped Yb/Er-doped $NaYF_4$ nanocrystals in toluene (0.5 wt %) measured using 980 nm diode laser (power density of 103 W/cm^2).

toluene. Under 980 nm laser excitation, the Er/Yb-doped $NaYF_4$ nanocrystals show three emission peaks near 520, 540, and 650 nm, which are respectively assigned to the $^2H_{11/2}$−$^4I_{15/2}$, $^4S_{3/2}$−$^4I_{15/2}$, and $^4F_{9/2}$−$^4I_{15/2}$ transitions. The origin of these emissions is from the excited energy levels of Er^{3+} ions, which are populated by multiple energy transfers from excited Yb^{3+} ions. The mechanism of the upconversion process is similar to that reported previously.[46−48] As

DOI: 10.1021/acs.langmuir.5b01070
Langmuir XXXX, XXX, XXX−XXX

mentioned earlier, the stability of the nanocrystals is not high due to the presence of methyl group near COO group. The weak binding of the MO molecules to the $NaYF_4$ nanocrystals causes slow settling of the nanocrystals in toluene. The idea is to take advantage of the weak binding of the ligand and exchange with strongly coordinating ligands and make the nanocrystals dispersion stable. First, to verify the feasibility of our idea, we exchange MO-capped nanocrystals with hydrophobic ligands such as oleic acid and oleylamine. After ligand exchange with these molecules, the nanocrystals were clearly dispersible in toluene. We then extended the ligand exchange strategy to hexanoic acid. The reason for choosing hexanoic acid is motivated by their low boiling point (~210 °C), which prevent it from using in thermal decomposition condition. After exchange with hexanoic acid, the nanocrystals were clearly dispersible in toluene. Figure 4 shows the comparisons of the

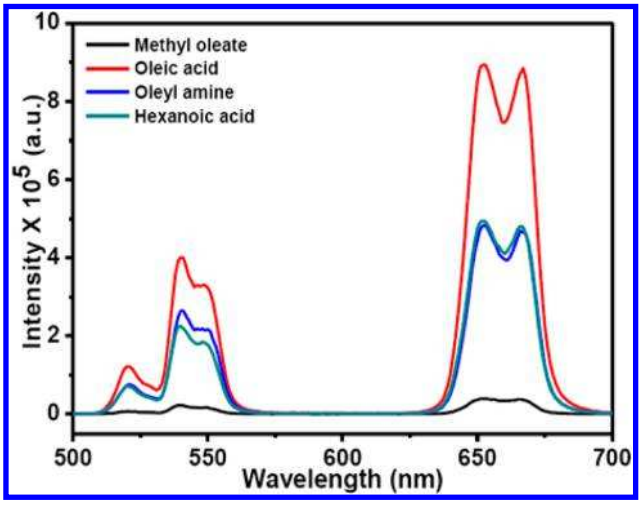

Figure 4. UC emission spectra of the MO-capped Yb/Er-doped $NaYF_4$ nanocrystals and the same after ligand exchange with oleic acid, oleylamine, and hexanoic acid in toluene. The laser power density is 103 W/cm^2.

upconversion emission spectra of the MO-capped Er/Yb-$NaYF_4$ nanocrystals in toluene and the same after ligand exchange with oleic acid, oleylamine, and hexanoic acid. Note that the higher emission intensities of the upconversion emission after ligand exchange compared to the MO-capped Er/Yb-doped $NaYF_4$ nanocrystals in toluene is likely due to difference in the stability between the nanocrystals. The UC emission intensity of the MO-capped nanocrystals decreases with time whereas the same after ligand exchange with oleic acid barely affected. Both oleylamine- and hexanoic acid-capped nanocrystals display a reasonably intense emission peak via upconversion process compared to MO-capped Er/Yb-doped $NaYF_4$ nanocrystals. This suggests the increase in the stability of the $NaYF_4$ nanocrystals after ligand exchange with oleic acid, oleylamine, and hexanoic acid. To make sure that no settling of particles during measurement, all samples were left undisturbed for 30 min before measurement. The presence of these ligands on the nanocrystals is confirmed by the FTIR and ^{1}H NMR analyses. Figure 5 shows FTIR spectra of MO capped Er/Yb-doped $NaYF_4$ nanocrystals after ligand exchange with oleic acid, hexanoic acid, and oleylamine. It is clear that after ligand exchange process the characteristic absorption band at 1746 cm^{-1} for C═O stretching of $COOCH_3$ group of methyl oleate molecules is absent. The new bands appear near 1717 and 1711

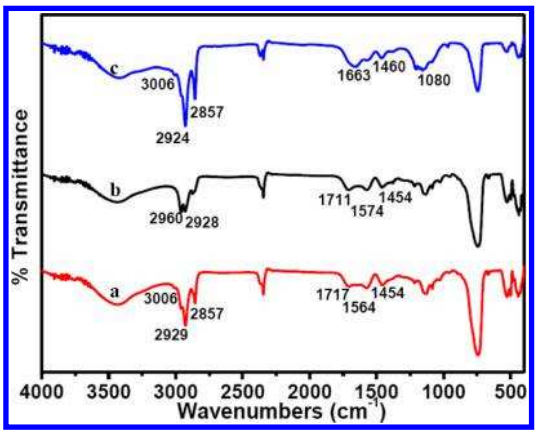

Figure 5. FTIR spectra of MO-capped Yb/Er-doped $NaYF_4$ nanocrystals after exchange with (a) oleic acid, (b) hexanoic acid, and (c) oleylamine.

cm^{-1} are due to the C═O stretching frequency of COOH group of oleic acid and hexanoic acid, respectively.[49] Two new bands appeared near 1574 and 1454 cm^{-1} which are assigned to the antisymmetric and symmetric vibration modes of the COO^- group. The attachment of oleylamine to the nanocrystals is verified by the presence of the peak at 1663 cm^{-1} due to the N−H bending of NH_2 group as well as due to the observed peak at 1080 cm^{-1} characteristic of C−N stretching ($-H_2C-NH_2$). These results indicate the adsorption of oleic acid/hexanoic acid/oleylamine onto the surface of the Er/Yb-doped $NaYF_4$ nanocrystals. The attachments of these ligands are further confirmed by ^{1}H NMR analysis. The ^{1}H NMR spectra of the methyl oleate-capped Er/Yb-doped $NaYF_4$ nanocrystals after exchange with oleic acid, hexanoic acid, and oleylamine are shown in Figures S6, S7, and S8 (Supporting Information). The appearance of CH protons of CH═CH near 5.31−5.33 ppm confirms the attachment of oleic acid molecules to the nanocrystals, while this peak is absent for the nanocrystals after ligand exchange with hexanoic acid molecules, suggesting the attachment of the latter. The appearance of the N−H proton at 2 ppm confirms that oleylamine has replaced the methyl oleate from the surface of the nanocrystals.

Having verified the feasibility of ligand exchange between methyl oleate-capped Er/Yb-doped $NaYF_4$ nanocrystals and hydrophobic ligands, the ligand exchange strategy was extended to ligands with hydrophilic groups at both ends. The reason for choosing dicarboxylic acid molecules as ligands for capping is due to the possibility of free COOH groups on the surface of the nanocrystals after the ligand exchange process to render the nanocrystals water dispersible. To this end, a series of dicarboxylic acids such as oxalic acid, malonic acid, succinic acid, adipic acid, and sebacic acid were ligand exchanged with MO-capped $NaYF_4$ nanocrystals. The attachment of these ligands (dicarboxylic acids) onto the surface of the nanocrystals is confirmed by the FTIR and ^{1}H NMR analyses. Figure 6 shows the FTIR spectra of methyl oleate-capped nanocrystals after ligand exchange with different dicarboxylic acid ligands. After the ligand exchange process with different dicarboxylic acids, the $NaYF_4$ nanocrystals display a peak near 1640 cm^{-1} due to the C═O stretching frequency of COO^- group along with a peak at 1730 cm^{-1}, which is ascribed to the C═O stretching frequency of free carboxylic acid groups. The attachment of oxalic acid to the surface of the nanocrystals after the ligand exchange process is confirmed by the absence of

DOI: 10.1021/acs.langmuir.5b01070
Langmuir XXXX, XXX, XXX−XXX

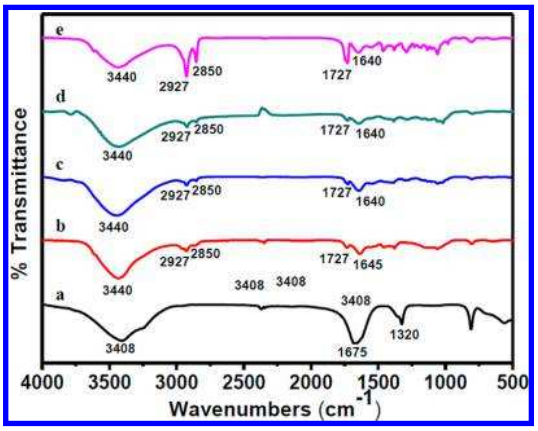

Figure 6. FTIR spectra of methyl oleate-capped Er/Yb-doped $NaYF_4$ nanocrystals after ligand exchange with (a) oxalic acid, (b) malonic acid, (c) succinic acid, (d) adipic acid, and (e) sebacic acid.

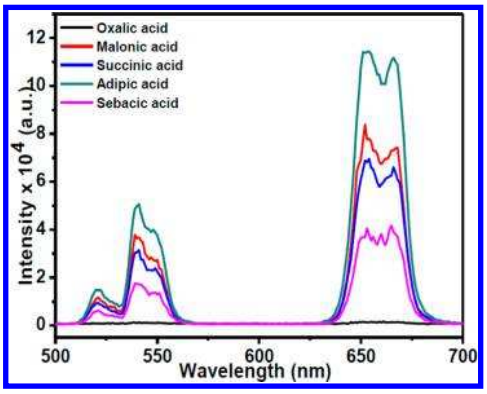

Figure 7. UC emission spectra of MO-capped Er/Yb-doped $NaYF_4$ nanocrystals after ligand exchange with dicarboxylic acids. The laser power density is 103 W/cm^2.

any characteristic C−H stretching vibrations near 2850 and 2927 cm^{-1} confirms the attachment of oxalic acid to the surface of the nanocrystals (see Figure 6a). In addition, binding of oxalic acid to the nanocrystals surface is verified by the observation of an intense peak near 1675 cm^{-1} which is assigned to the C═O stretching frequency of the COOH group. In addition to FTIR analysis, the ^1H NMR measurements of these nanocrystals also confirm the ligand exchange reaction. The ^1H NMR spectra of the MO-capped Er/Yb-doped $NaYF_4$ nanocrystals after exchange with oxalic acid, malonic acid, succinic acid, adipic acid, and sebacic acid are shown in Figures S9−S13 (Supporting Information). The absence of CH proton of CH═CH appearing between 5.31 and 5.33 ppm and the appearance of CH_2 proton peaks confirm that ligand exchange has occurred. For the methyl oleate-capped nanocrystals after ligand exchange with oxalic acid, no proton signals were observed. This is expected as oxalic acid capping lead to deprotonation of both protons.

The binding of malonic acid, succinic acid, adipic acid, and sebacic acid onto the surface of the nanocrystals is also supported by the improved dispersibility of the nanocrystals in water due to the presence of COOH groups near the surface. The high water dispersibility after ligand exchange with dicarboxylic acid molecules led to intense upconversion emission peaks from the nanocrystals. The upconversion emission spectra of the dicarboxylic acid-capped Er/Yb-doped $NaYF_4$nanocrystals (via ligand exchange) are shown in Figure 7. It is important to note that the malonic acid, succinic acid, adipic acid, and sebacic acid coated nanocrystals are quite stable in water and display strong luminescence. The relatively strong emission intensity noted for the adipic acid-capped Er/Yb-doped $NaYF_4$ nanocrystals is presumably due to the high stability of nanocrystals caused by the balance between the hydrophobic and hydrophilic interactions. However, oxalic acid-coated nanocrystals display weak luminescence and poor dispersibility in water, which is likely due to the lack of free COOH to render the nanocrystal's surface hydrophilic. The comparatively lower stability observed for the sebacic acid-capped $NaYF_4$ nanocrystals is due to the increase in the hydrophobic interaction between the methylene units. To understand the effect of water, the luminescence properties of dicarboxylic acid-coated nanocrystals were measured in D_2O. Figure S14 shows the upconversion emission spectra of the dicarboxylic acid-capped Er/Yb-doped $NaYF_4$ nanocrystals (via ligand exchange) in D_2O. For all dicarboxylate-capped nanocrystals, the observed green to red emission intensity ratio (G/R) is almost close to 0.46 in D_2O. This value is slightly decreased compared to that the same measured in water (0.35). The decrease in the G/R in water is attributed to the isotopic effect. We believe that the energy difference between the green emitting level ($^4S_{3/2}$) and the red emitting level ($^4F_{9/2}$) is ∼3050 cm^{-1} which can be easily match with the O−H vibrations, thereby increasing the population of the red emitting level. To understand the effect of different refractive indices on the emission, we have measured luminescence measurements in different solvents, i.e., DMSO (1.47), DMF (1.43), ethanol (1.36). The refractive index values of the solvents are given in parentheses. Figure S15 shows the upconversion emission spectra of the adipic acid-coated Er/Yb-doped $NaYF_4$ nanocrystals in DMSO, DMF, and ethanol. It is evident from the spectra that the observed G/R (0.23) for adipic acid-coated nanocrystals in DMSO, DMF, and ethanol are quite similar. It suggests that there is barely any effect of refractive index of the solvents on the G/R of the capped nanocrystals.

A time-dependent UC emission measurements were performed to understand the stability of the adipic acid-coated nanocrystals in water. It is clear from the emission spectra shown in Figure S16 (see Supporting Information) that the Er/Yb-doped $NaYF_4$ nanocrystals coated with adipic acid are quite stable for 15 h but show a slight reduction in the intensity after 24 h. The reason for the decrease in the intensity is presumably due to slow settling of the nanocrystals caused by the interaction between the methylene groups in adipic acid.

To evaluate the stability of the nanocrystals under photo-excitation, we performed the photoluminescence measurements of the dicarboxlic acid-functionalized Er/Yb-doped $NaYF_4$ nanocrystals (via ligand exchange) under continuous exposure to a 980 nm laser. Figure S17 shows the plot of upconversion emission intensities after continuous laser irradiation of the nanocrystals for 12 h. The results suggest absence of any significant change in the luminescence intensity of the nanocrystals, suggesting the high photostability of the dicarboxylic acid-capped Er/Yb-doped $NaYF_4$ nanocrystals. We then extended the study to understand the stability of the ligand exchanged nanocrystals in different biological medium such as water at different pH, cell culture medium, and PBS buffer. This is done by measuring the upconversion luminescence intensity as well as DLS analysis for about 14 days. The results of these measurements suggest only a slight change in the average hydrodynamic diameter as well as in the

DOI: 10.1021/acs.langmuir.5b01070
Langmuir XXXX, XXX, XXX−XXX

luminescence intensity. At pH < 7 the hydrodynamic diameter and luminescence were unaffected, but at pH > 7 we observed a slight increase in the average hydrodynamic size of the nanocrystals with a concomitant decrease in the upconversion emission intensity (Figure S18). This suggests a likely aggregation of the nanocrystals, which could lead to self-quenching of the luminescence. In the case of dicarboxylic acid-capped nanocrystals in cell culture medium, both hydrodynamic diameter and fluorescence intensity were unaffected over 14 days (Figure S19). But in the case of nanocrystals dispersed in PBS buffer, the hydrodynamic diameter slightly increases with an associated decrease in the fluorescence intensity presumably due to aggregation (Figure S20).

To check the effect of ligands on the emission lifetime of Er^{3+} ions, we have performed lifetime measurements for all ligands under 488 nm excitation after ligand exchange. Figure S21 shows the average emission lifetime measurements of the green emission of Er^{3+} ions in Er/Yb-doped $NaYF_4$ nanocrystals under 488 nm excitation for the dicarboxylic acids. The observed lifetime values are 174, 182, 178, and 171 μs respectively for malonic, succinic, adipic, and sebacic acids. These lifetime values vary only slightly within the series as well as slightly longer compared to the methyl oleate-capped nanocrystals. This is reasonable as these nanocrystals are prepared through ligand exchange there is barely any change in the size and phase of the nanocrystals. The only aspect that could affect the lifetime is the nonradiative relaxation due to the difference in the ligands. However, this effect will be minimum as the particles are larger in size and most of the Er^{3+} ions are expected to reside at the core. In addition, the 4f energy levels are less affected by the ligand field. Although the ligand attachment did not affect the lifetimes much, the stabilities of the particles are higher after ligand exchange compared to methyl oleate-capped nanocrystals.

To study the effect of ionic strength on the stability of the dicarboxylic acid nanocrystals, we choose adipic acid-capped nanocrystals (as it contains more methylene units next to sebacic acid). We prepared four different concentrations 0.3. 0.5, 1.0, and 2 wt % of nanocrystal dispersions and measured their luminescence just after preparation (1 min) and after 30 min. The results shown in Figure S22 clearly indicate that the nanocrystal dispersions are stable up to 2 wt % concentration. After 30 min, the lower concentration samples display a slight decrease in the intensity whereas effect is relatively larger in the case of 2 wt % sample.

Finally, to confirm that the phase and the average size of the nanocrystals are preserved after the ligand exchange process with dicarboxylic acids, both XRD and TEM measurements were done. The XRD patterns of the nanocrystals after the ligand exchange process are shown in Figure 8. The patterns match with the standard pattern of cubic $NaYF_4$, confirming that the phase of the nanocrystals are not affected after ligand exchange process. Similarly, the TEM images of the nanocrystals after ligand exchange process confirm that the particle size and shape are preserved (see Figure S23 in Supporting Information).

To find the mechanism involved in the ligand exchange process, we took adipic acid as a case study. In the case of ligand exchange process with adipic acid, the FTIR spectrum of the residue (collected in diethyl ether layer) matched well with the FTIR spectrum of pure oleic acid (Figure S24). We believe that during sonication the weakly attached methyl oleate ligands break into oleic acid, which is recovered in diethyl ether.

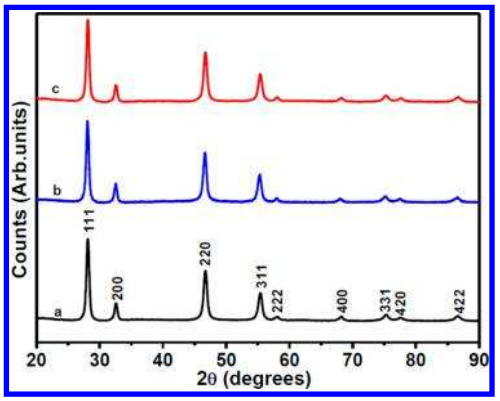

Figure 8. XRD patterns of MO-capped Yb/Er-doped $NaYF_4$ nanocrystals after ligand exchanged with (a) malonic acid, (b) succinic acid, and (c) adipic acid.

Although the presence of oleic acid in the mixture could compete with adipic acid molecules to bind to the surface of the nanocrystals, the lower solubility of oleic acid in water leads to preferential attachment of adipic acid to the nanocrystals surface (the exchange process was carried out in water). Whereas in the case of ligand exchange with hydrophobic ligands such as oleic acid, the experiment was carried out in hexane which led to the attachment of oleic acid molecules.

4. CONCLUSIONS

We have described a versatile ligand-exchange strategy to modify the surface of the nanocrystals both hydrophilic and hydrophobic by simple sonication without affecting the particle size, shape, and phase. This is achieved by first preparing Er/Yb-doped $NaYF_4$ nanocrystals capped with weakly binding ligands such as methyl oleate. A simple ligand exchange process with molecules like oleic acid, oleylamine, and hexanoic acid resulted in the corresponding ligand stabilized nanocrystals. We emphasize that direct attachment of hexanoic acid to the nanocrystals is difficult via thermal decomposition method due to their low boiling point. Similarly, the ligand exchange was achieved with dicarboxylic acid ligands such as malonic acid, succinic acid, adipic acid, etc., to make water-dispersible nanocrystals. The driving force for the reaction is the stabilizing of the nanocrystal with weak ligand such as methyl oleate compared to the oleic acid or dicarboxylic acids which bind strongly to the surface of the nanocrystals. The advantage of the present approach is the capping of nanocrystals with ligands which possess low boiling point which are otherwise difficult to prepare with high temperature thermal decomposition method. We strongly believe that this ligand exchange strategy can easily be extended to prepare nanocrystals with a variety of ligands.

■ ASSOCIATED CONTENT

Ⓢ Supporting Information

NMR spectra, time-dependent upconversion emission spectra at different biological medium, DLS measurements, FTIR results, lifetime graph, TEM images of nanocrystals after ligand exchanged with hexanoic acid, adipic acid, and sebacic acid. The Supporting Information is available free of charge on the ACS Publications website at DOI: 10.1021/acs.langmuir.5b01070.

■ AUTHOR INFORMATION

Corresponding Author

*E-mail mvenkataramanan@yahoo.com (V.M.).

DOI: 10.1021/acs.langmuir.5b01070
Langmuir XXXX, XXX, XXX−XXX

Notes

The authors declare no competing financial interest.

■ ACKNOWLEDGMENTS

V.M. thanks CSIR for the project 01(2716)13 and Indian Institute of Science Education and Research (IISER), Kolkata, for the funding. B.M. and V.N.K.B.A. thank IISER Kolkata and UGC, respectively, for funding.

■ REFERENCES

(1) Eliseeva, S. V.; Bünzli, J. C. G. Lanthanide Luminescence for Functional Materials and Bio-sciences. *Chem. Soc. Rev.* **2010**, *39*, 189−227.
(2) Vetrone, F.; Boyer, J. C.; Capobianco, J. A. In *The Handbook of Luminescence, Display Materials and Devices*; Rohwer, L. S., Nalwa, H. S., Eds.; American Scientific Publishers: Los Angeles, 2003.
(3) Binnemans, K. Lanthanide-Based Luminescent Hybrid Materials. *Chem. Rev.* **2009**, *109*, 4283−4374.
(4) Sarkar, S.; Meesaragandla, B.; Hazra, C.; Mahalingam, V. A Platform to Realize Upconversion via Interparticle Energy Transfer. *Adv. Mater.* **2013**, *25*, 856−860.
(5) Eliseeva, S. V.; Bünzli, J.-C. G. Intriguing Aspects of Lanthanide Luminescence. *Chem. Sci.* **2013**, *4*, 1939−1949.
(6) Im, W. B.; George, N.; Kurzman, J.; Brinkley, S.; Mikhailovsky, A.; Hu, J.; Chmelka, B. F.; DenBaars, S. P.; Seshadri, R. Efficient and Color-Tunable Oxyfluoride Solid Solution Phosphors for Solid-State White Lighting. *Adv. Mater.* **2011**, *23*, 2300−2305.
(7) Anikeeva, P. O.; Halpert, J. E.; Bawendi, M. G.; Bulovic, V. Electroluminescence from a Mixed Red−Green−Blue Colloidal Quantum Dot Monolayer. *Nano Lett.* **2007**, *7*, 82196.
(8) Park, J. K.; Choi, K. J.; Yeon, J. H.; Lee, S. J.; Kim, C. H. Embodiment of the warm white-light-emitting diodes by using a Ba^{2+}codoped Sr_3SiO_5:Eu phosphor. *Appl. Phys. Lett.* **2006**, *88*, 043511.
(9) Trupke, T.; Green, M. A.; Wurfel, P. Improving Solar Cell Efficiencies by Up-conversion of Sub-Band-Gap Light. *J. Appl. Phys.* **2002**, *92*, 4117−4122.
(10) Van der Ende, B. M.; Aarts, L.; Meijerink, A. Lanthanide Ions As Spectral Converters for Solar Cells. *Phys. Chem. Chem. Phys.* **2009**, *11*, 11081−11095.
(11) Shalav, A.; Richards, B. S.; Green, M. A. Luminescent Layers for Enhanced Silicon Solar Cell Performance: Up-conversion. *Sol. Energy Mater. Sol. Cells* **2007**, *91*, 829−842.
(12) Chatterjee, D. K.; Fong, L. S.; Zhang, Y. Nanoparticles in Photodynamic Therapy: An Emerging Paradigm. *Adv. Drug Delivery Rev.* **2008**, *60*, 1627−1637.
(13) Yang, D.; Ma, P.; Hou, Z.; Cheng, Z.; Li, C.; Lin, J. Current Advances in Lanthanide Ion (Ln^{3+})-Based Upconversion Nanomaterials for Drug Delivery. *Chem. Soc. Rev.* **2015**, *44*, 1416−1448.
(14) Auzel, F. Upconversion and Anti-Stokes Processes with f and d Ions in Solids. *Chem. Rev.* **2004**, *104*, 139−173.
(15) Haase, M.; Schafer, H. Upconverting Nanoparticles. *Angew. Chem., Int. Ed.* **2011**, *50*, 5808−5829.
(16) Wang, J.; Wang, F.; Wang, C.; Liu, Z.; Liu, X. Single-Band Upconversion Emission in Lanthanide-Doped $KMnF_3$Nanocrystals. *Angew. Chem., Int. Ed.* **2011**, *50*, 10369−10372.
(17) Wang, F.; Han, Y.; Lim, C. S.; Lu, Y.; Wang, J.; Xu, J.; Chen, H.; Zhang, C.; Hong, M.; Liu, X. Simultaneous Phase and Size Control of Upconversion Nanocrystals through Lanthanide Doping. *Nature* **2010**, *463*, 1061−1065.
(18) Teng, X.; Zhu, Y.; Wei, W.; Wang, S.; Huang, J.; Naccache, R.; Hu, W.; Tok, A. I. Y.; Han, Y.; Zhang, Q.; Fan, Q.; Huang, W.; Capobianco, J. A.; Huang, L. Lanthanide-Doped Na_xScF_{3+x} Nanocrystals: Crystal Structure Evolution and Multicolor Tuning. *J. Am. Chem. Soc.* **2012**, *134*, 8340−8343.
(19) Mader, H. S.; Kele, P.; Saleh, S. M.; Wolfbeis, O. S. Upconverting Luminescent Nanoparticles for Use in Bioconjugation and Bioimaging. *Curr. Opin. Chem. Biol.* **2010**, *14*, 582−596.
(20) Wang, F.; Banerjee, D.; Liu, Y.; Chen, X.; Liu, X. Upconversion Nanoparticles in Biological Labeling, Imaging, and Therapy. *Analyst* **2010**, *135*, 1839−1854.
(21) Pichaandi, J.; Boyer, J. C.; Delaney, K. R.; van Veggel, F. C. J. M. Two-Photon Upconversion Laser (Scanning and Wide-Field) Microscopy Using Ln^{3+}-Doped $NaYF_4$ Upconverting Nanocrystals: A Critical Evaluation of their Performance and Potential in Bioimaging. *J. Phys. Chem. C* **2011**, *115*, 19054−19064.
(22) Chatterjee, D. K.; Gnanasammandhan, M. K.; Zhang, Y. Small Upconverting Fluorescent Nanoparticles for Biomedical Applications. *Small* **2010**, *24*, 2781−2795.
(23) Priyam, M.; Idris, N. M.; Zhang, Y. Gold Nanoshell Coated $NaYF_4$ Nanoparticles for Simultaneously Enhanced Upconversion Fluorescence and Darkfield Imaging. *J. Mater. Chem.* **2012**, *22*, 960−965.
(24) Mahalingam, V.; Vetrone, F.; Naccache, R.; Speghini, A.; Capobianco, J. A. Structural and Optical Investigation of Colloidal Ln^{3+}/Yb^{3+} Co-doped KY_3F_{10} Nanocrystals. *J. Mater. Chem.* **2009**, *19*, 3149−3152.
(25) Chai, R. T.; Lian, H. Z.; Hou, Z. Y.; Zhang, C. M.; Peng, C.; Lin, J. Preparation and Characterization of Upconversion Luminescent $NaYF_4$:Yb^{3+}, Er^{3+} (Tm^{3+})/PMMA Bulk Transparent Nanocomposites Through In Situ Photopolymerization. *J. Phys. Chem. C* **2010**, *114*, 610−616.
(26) Boyer, J. C.; Johnson, N. J. J.; van Veggel, F. C. J. M. Upconverting Lanthanide-Doped $NaYF_4$-PMMA Polymer Composites Prepared by in Situ Polymerization. *Chem. Mater.* **2009**, *21*, 2010−2012.
(27) Sarkar, S.; Hazra, C.; Mahalingam, V. Bright Luminescence from Colloidal Ln^{3+}-Doped $Ca_{0.72}Y_{0.28}F_{2.28}$ (Ln = Eu, Tm/Yb) Nanocrystals via Both High and Low Energy Radiations. *Chem.—Eur. J.* **2012**, *18*, 7050−7054.
(28) Mahalingam, V.; Vetrone, F.; Naccache, R.; Speghini, A.; Capobianco, J. A. Colloidal Tm^{3+}/Yb^{3+}-Doped LiYF4 Nanocrystals: Multiple Luminescence Spanning the UV to NIR Regions via Low-Energy Excitation. *Adv. Mater.* **2009**, *21*, 4025−4028.
(29) Wang, H. Q.; Nann, T. Monodisperse Upconverting Nanocrystals by Microwave-Assisted Synthesis. *ACS Nano* **2009**, *3*, 3804−3808.
(30) Wang, L.; Li, Y. Controlled Synthesis and Luminescence of Lanthanide Doped $NaYF_4$ Nanocrystals. *Chem. Mater.* **2007**, *19*, 727−734.
(31) Wang, J.; Wang, F.; Wang, C.; Liu, Z.; Liu, X. Single-Band Upconversion Emission in Lanthanide-Doped $KMnF_3$ Nanocrystals. *Angew. Chem., Int. Ed.* **2011**, *50*, 10369−10372.
(32) Meesaragandla, B.; Shyam Sarkar, S.; Hazra, C.; Mahalingam, V. Ricinoleic Acid-Capped Upconverting Nanocrystals: An Ideal Capping Ligand to Render Nanocrystals Water Dispersible. *ChemPlusChem* **2013**, *78*, 1338−1342.
(33) Xingchen Ye, X.; Collins, J. E.; Kang, Y.; Chen, J.; Chen, D. T. N.; Yodh, A. G.; Murray, C. B. Morphologically Controlled Synthesis of Colloidal Upconversion Nanophosphors and Their Shape-Directed Self-Assembly. *Proc. Natl. Acad. Sci. U. S. A.* **2010**, *107*, 22430−22435.
(34) Boyer, J. C.; Vetrone, F.; Cuccia, L. A.; Capobianco, J. A. Synthesis of Colloidal Upconverting $NaYF_4$: Er^{3+}/Yb^{3+} and Tm^{3+}/Yb^{3+} Monodisperse Nanocrystals. *Nano Lett.* **2007**, *7*, 847−852.
(35) Yi, G.-S.; Chow, G.-M. Water-Soluble $NaYF_4$:Yb,Er(Tm)/$NaYF_4$/Polymer Core/Shell/Shell Nanoparticles with Significant Enhancement of Upconversion Fluorescence. *Chem. Mater.* **2007**, *19*, 341−343.
(36) Jalil, R. A.; Zhang, Y. Biocompatibility of Silica Coated $NaYF_4$ Upconversion Fluorescent Nanocrystals. *Biomaterials* **2008**, *29*, 4122−4128.
(37) Chen, Z.; Chen, H.; Hu, H.; Yu, M.; Li, F.; Zhang, Q.; Zhou, Z.; Yi, T.; Huang, C. Versatile Synthesis Strategy for Carboxylic Acid-functionalized Upconverting Nanophosphors as Biological Labels. *J. Am. Chem. Soc.* **2008**, *130*, 3023−3029.
(38) Naccache, R.; Vetrone, F.; Mahalingam, V.; Cuccia, L. A.; Capobianco, J. A. Controlled Synthesis and Water Dispersibility of

DOI: 10.1021/acs.langmuir.5b01070
Langmuir XXXX, XXX, XXX−XXX

Hexagonal Phase $NaGdF_4$:Ho^{3+}/Yb^{3+} Nanoparticles. *Chem. Mater.* **2009**, *21*, 717−723.
(39) Bogdan, N.; Vetrone, F.; Ozin, G. A.; Capobianco, J. A. Synthesis of Ligand-Free Colloidally Stable Water Dispersible Brightly Luminescent Lanthanide-Doped Upconverting Nanoparticles. *Nano Lett.* **2011**, *11*, 835−840.
(40) Johnson, J. J.; Sangeetha, N. M.; Boyer, J. C.; van Veggel, F. C. J. M. Facile Ligand-Exchange with Polyvinylpyrrolidone and Subsequent Silica Coating of Hydrophobic Upconverting b-NaYF4:Yb^{3+}/Er^{3+} Nanoparticles. *Nanoscale* **2010**, *2*, 771−777.
(41) Zhang, T.; Ge, J.; Hu, Y.; Yin, Y. A General Approach for Transferring Hydrophobic Nanocrystals into Water. *Nano Lett.* **2007**, *7*, 3203−3207.
(42) Nyk, M.; Kumar, R.; Ohulchanskyy, T. Y.; Bergey, E. J.; Prasad, P. N. High Contrast in Vitro and in Vivo Photoluminescence Bioimaging Using Near Infrared to Near Infrared Up-Conversion in Tm3+ and Yb3+ Doped Fluoride Nanophosphors. *Nano Lett.* **2008**, *8*, 3834−3838.
(43) Dong, A.; Ye, X.; Chen, J.; Kang, Y.; Gordon, T.; Kikkawa, J. M.; Murray, C. B. A Generalized Ligand-Exchange Strategy Enabling Sequential Surface Functionalization of Colloidal Nanocrystals. *J. Am. Chem. Soc.* **2011**, *133*, 998−1006.
(44) Boyer, J. C.; Vetrone, F.; Cuccia, L. A.; Capobianco, J. A. Synthesis of Colloidal Upconverting $NaYF_4$ Nanocrystals Doped with Er^{3+}, Yb^{3+} and Tm^{3+}, Yb^{3+} via Thermal Decomposition of Lanthanide Trifluoroacetate Precursors. *J. Am. Chem. Soc.* **2006**, *128*, 7444−7445.
(45) Zhang, Y. W.; Sun, X.; Si, R.; You, L.; Yan, C. Single-Crystalline and Monodisperse LaF_3 Triangular Nanoplates from a Single-Source Precursor. *J. Am. Chem. Soc.* **2005**, *127*, 3260−3261.
(46) Krämer, K. W.; Biner, D.; Frei, G.; Güdel, H. U.; Hehlen, M. P.; Lüthi, S. R. Hexagonal Sodium Yttrium Fluoride Based Green and Blue Emitting Upconversion Phosphors. *Chem. Mater.* **2004**, *16*, 1244−1251.
(47) Wang, F.; Liu, X. G. Recent Advances in the Chemistry of Lanthanide-Doped Upconversion Nanocrystals. *Chem. Soc. Rev.* **2009**, *38*, 976−989.
(48) Zhao, J.; Lu, Z.; Yin, Y.; McRae, C.; Piper, J. A.; Dawes, J. M.; Jin, D.; Goldysa, E. M. Upconversion Luminescence with Tunable Lifetime in $NaYF_4$:Yb,Er Nanocrystals: Role of Nanocrystal Size. *Nanoscale* **2013**, *5*, 944−952.
(49) Chaput, F.; Lerouge, F.; Nenez, S. T.; Coulon, P. E.; Dujardin, C.; Quanquin, S. D.; Mpambani, F.; Parola, S. Rare Earth Fluoride Nanoparticles Obtained Using Charge Transfer Complexes: A Versatile and Efficient Route Toward Colloidal Suspensions and Monolithic Transparent Xerogels. *Langmuir* **2011**, *27*, 5555−5561.

DOI: 10.1021/acs.langmuir.5b01070
Langmuir XXXX, XXX, XXX−XXX